

Resist-based measurement of the contrast transfer function in a 0.3 numerical aperture extreme ultraviolet microfield optic

Jason P. Cain^{a)}

Department of Electrical Engineering and Computer Sciences, University of California, Berkeley, California 94720

Patrick Naulleau

College of Nanoscale Science and Engineering, University at Albany, Albany, New York 12203

Costas J. Spanos

Department of Electrical Engineering and Computer Sciences, University of California, Berkeley, California 94720

(Received 28 July 2005; accepted 5 December 2005; published 25 January 2006)

In order to meet the high-resolution printing potential of extreme ultraviolet (EUV) lithography, the projection optics must be of very high quality. The contrast transfer function (CTF), a measure of the aerial-image contrast as a function of pitch, describes one key aspect of projection optic quality. In order to support research into EUV lithography, a static microfield exposure tool (MET) based on a 0.3 numerical aperture optic and operating at a wavelength of 13.5 nm has been developed at the Advanced Light Source, a synchrotron facility at the Lawrence Berkeley National Laboratory. This work presents the results of resist-based measurements of the CTF for the MET optic. Although the resist is not an ideal aerial-image detector due to its nonlinear response, it is still possible to study some key characteristics of the optics using such methods. These measurements are based on line/space patterns printed in several different EUV photoresists. The experimental CTF results are compared with the CTF from aerial-image simulations including the aberrations measured in the projection optic using interferometric and lithographic techniques. The measured CTF values are found to be significantly lower than predicted from the aerial-image simulations. CTF measurements are presented for both bright-field and dark-field mask patterns in order to investigate the effect of flare. Finally, the orientation dependence of the CTF is studied in order to evaluate the effect of nonrotationally symmetric lens aberrations. Neither flare nor nonrotationally symmetric aberrations were found to have a significant effect on the measured CTF. Photoresist resolution is believed to be the limiting factor in the observed contrast transfer function. These measurements, taken as a whole, provide valuable information about the imaging performance of the MET optic and aid in interpreting the results of other experiments performed using the MET and similar systems. © 2006 American Vacuum Society. [DOI: 10.1116/1.2162578]

I. INTRODUCTION

Extreme ultraviolet (EUV) lithography at a wavelength near 13.5 nm is under development as a next-generation lithography technology for use in semiconductor manufacturing. Although EUV lithography offers great benefits in terms of resolution, there are a number of challenges involved that must be overcome if the technology is to see production use (currently targeted for the 32 nm technology node).

In order to support EUV lithography research and development to address these issues, a static microfield exposure tool based on the microexposure tool (MET) optic design and operating at a wavelength of 13.5 nm has been installed at the Advanced Light Source, a synchrotron facility at the Lawrence Berkeley National Laboratory.¹⁻³ The MET optic is composed of two multilayer-coated reflective elements and has a numerical aperture (NA) of 0.3, slightly larger than the value expected for first-generation EUV production tools. The field size is $600 \times 200 \mu\text{m}^2$ at the wafer (demagnified by

a factor of $5\times$ from the object plane), and the tool uses a scanning illuminator to provide programmable coherence control.⁴

Extremely high optical quality is required for all lithography systems, and this is particularly true in EUV lithography as the short illumination wavelength means that wave-front errors of even 1 nm may lead to significant degradation of the aerial image. One of the most important properties of a projection optical system is its ability to transfer contrast from the object (mask) plane to the image (wafer) plane. This property is often characterized using the contrast transfer function (CTF). The CTF is closely related to the modulation transfer function (MTF), which itself is directly related to the pupil function.⁵ In this article, the CTF for the MET optic is measured using a photoresist-based technique as a means of quantifying optical performance as a function of pitch. The measurement technique is described in Sec. II. Simulation of the CTF in order to establish expected performance is discussed in Sec. III, while measured results for several different photoresists are presented in Sec. IV. A comparison of CTF measurements made using bright-field and

^{a)}Electronic mail: jason.cain@amd.com

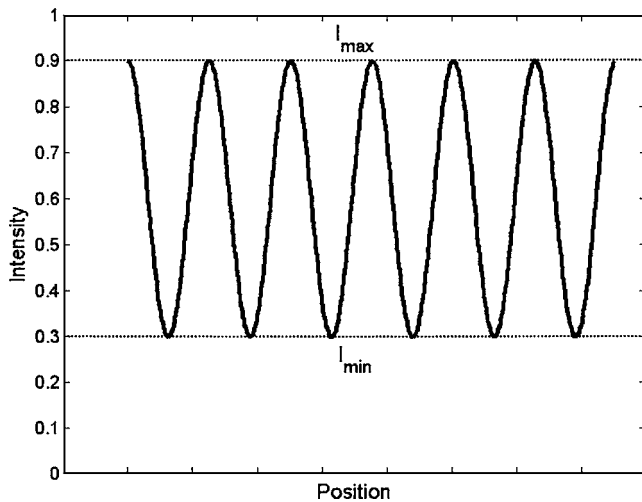


FIG. 1. Illustration of factors determining aerial-image contrast.

dark-field mask patterns is given in Sec. V, and orientation dependence of the CTF measurements is addressed in Sec. VI. Finally, conclusions are presented in Sec. VII.

II. MEASUREMENT OF AERIAL-IMAGE CONTRAST

One important factor in determining the photoresist printing performance of an aerial image projected by a lithography tool is the image contrast, defined as

$$\text{contrast} = \frac{I_{\max} - I_{\min}}{I_{\max} + I_{\min}}, \quad (1)$$

where I_{\max} and I_{\min} are the maximum and minimum aerial-image intensities, respectively (Fig. 1). Aerial-image contrast is a function of feature size or, equivalently, of spatial frequency. For features with dimensions that are large relative to the exposure wavelength, the image contrast should ideally be unity, whereas for small features beyond the resolution limit of the optical system the contrast will be zero. The details of the transition between these two extremes depend on the parameters of the optical system, including numerical aperture, wave-front quality, illumination wavelength, and partial coherence. This dependence on feature size brings about the concept of the CTF, a mapping of feature size or spatial frequency to the corresponding image contrast.

Direct measurement of aerial-image contrast is difficult. In this work a photoresist threshold technique^{6,7} is utilized to measure I_{\max} and I_{\min} , and the image contrast is calculated from these two values. This process is illustrated for the case of positive resists in Fig. 2. As the exposure dose is increased from Fig. 2(a) to Fig. 2(c), the postdevelop linewidth shrinks (here a simple resist threshold model of development is assumed). Therefore, I_{\max} occurs at the exposure dose (D_{\max}) at which individual lines first become evident in the resist while I_{\min} occurs at the dose (D_{\min}) at which the lines vanish completely and the resist is dissolved completely by the developer. Therefore, the measured contrast may be expressed as

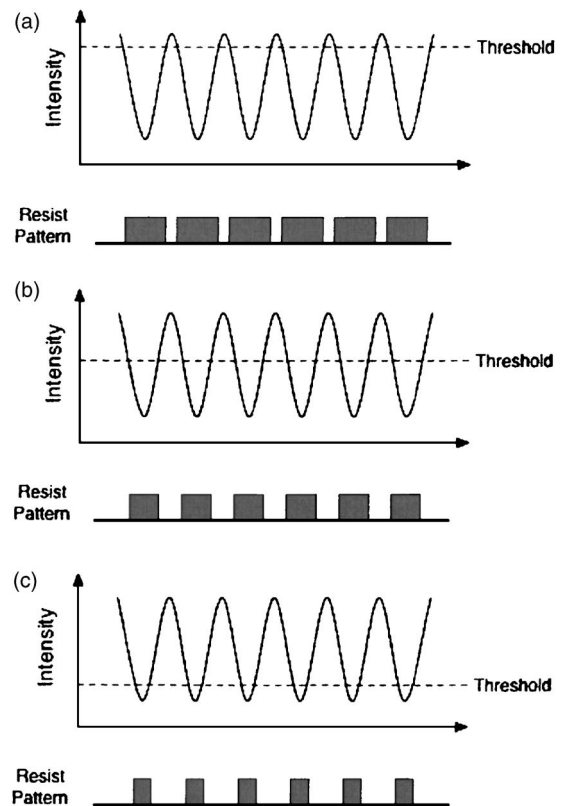


FIG. 2. Principle of contrast measurement in photoresist. As the exposure dose is increased from (a) to (c), the developed linewidth shrinks for positive resists.

$$\text{contrast} = \frac{D_{\max} - D_{\min}}{D_{\max} + D_{\min}}. \quad (2)$$

Example resist images at dose levels D_{\max} and D_{\min} are shown in Fig. 3. Measurement of the contrast over a range of feature sizes allows for reconstruction of the CTF.

III. SIMULATION OF CONTRAST TRANSFER FUNCTION FOR THE MET OPTIC

The expected CTF for an optical system can be obtained through simulation provided that the important system parameters, including wave-front information and illumination conditions, are known. The expected CTF for the MET system was simulated using the PROLITH software package. In this case the lateral-shearing interferometry (LSI) measurements of the MET optic wave front⁸ were combined with lithographic measurements of key aberration terms (astigmatism and spherical aberration) to accurately model the impact of aberrations on the CTF. The wave-front data for the center of the field were used, as this is where the measurements were performed. In addition, the amount of flare present in the system was predicted using surface roughness measurements of the optical elements of the MET. This predicted flare was also included in the simulations. Annular illumination was used for both simulation and experiments, with $\sigma_{\text{inner}}=0.3$ and $\sigma_{\text{outer}}=0.7$. The simulated CTF for vertical lines is shown in Fig. 4 for both the ideal (unaberrated) and

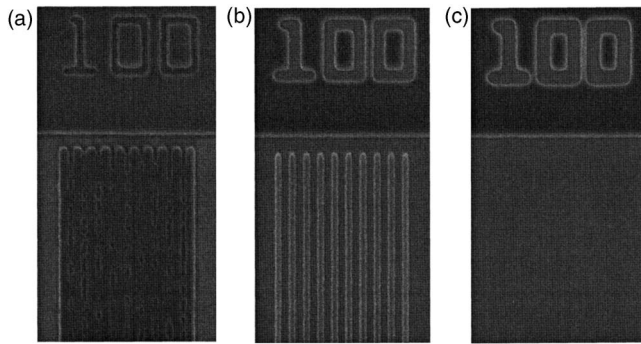


FIG. 3. Postdevelop resist patterns in Rohm and Haas EUV-2D resist for 100 nm features corresponding to exposure dose of (a) D_{\max} , (b) midpoint between D_{\max} and D_{\min} , and (c) D_{\min} .

aberrated cases. The results show clearly that aberrations and flare have a strong impact on the image contrast, particularly for smaller feature sizes.

IV. DARK-FIELD CONTRAST TRANSFER FUNCTION MEASUREMENTS

The CTF for the MET was first measured experimentally using a dark-field mask, meaning that the majority of the mask area is covered with an absorber layer. Three resists were used: Rohm and Haas EUV-2D, Rohm and Haas MET-1K (XP 3454C), and a ketal resist system (KRS).⁹ A resist thickness of 125 nm was used in each case. The post-application bake (PAB) and postexposure bake (PEB) temperatures for EUV-2D and MET-1K were both 130 °C, while KRS does not require a PEB step. Annular illumination was used, with $\sigma_{\text{inner}}=0.3$ and $\sigma_{\text{outer}}=0.7$. These exposure conditions were chosen to be representative of typical printing conditions. The mask pattern contained vertical lines and spaces of equal width ranging from 20 to 120 nm (wafer dimensions). The measurement results for the center of the field are shown in Fig. 5.

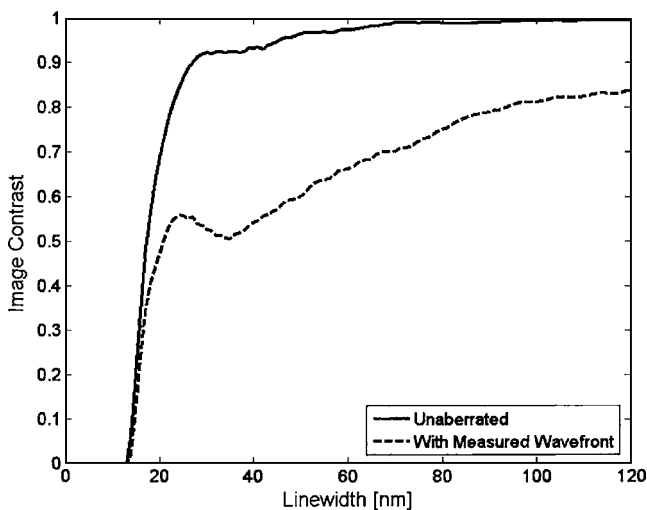


FIG. 4. Simulated contrast transfer function for the MET optic under ideal, unaberrated conditions (solid line) and using the aberrated wave front as measured using lateral shearing interferometry (dashed line).

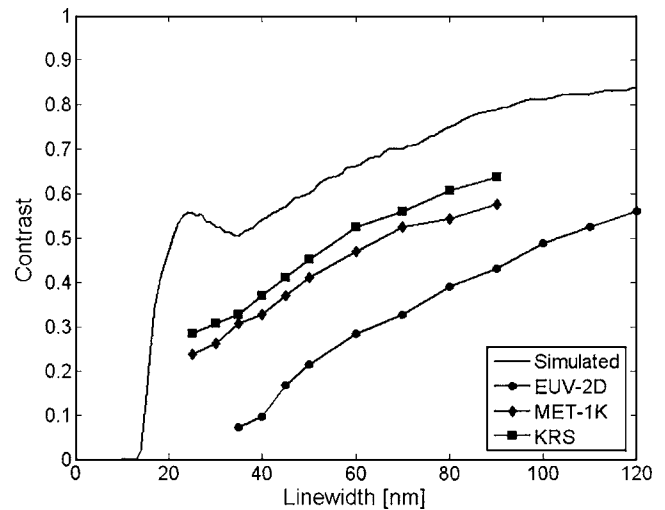


FIG. 5. Contrast transfer function for the MET optic. Simulation results (including effects of aberrated wave front) are shown along with measurements for three different resists: Rohm and Haas EUV-2D, Rohm and Haas MET-1K (XP 3454C), and a derivative of the KRS resist formulation.

The dark-field CTF measurements show a clear dependence on the type of resist used. The apparent CTF for EUV-2D is significantly lower than for MET-1K and KRS. This is consistent with previous results, which suggest that the resolution limit for EUV-2D occurs at larger feature sizes than for MET-1K.³ Recent results also suggest that this particular formulation of KRS has a resolution comparable to that of MET-1K.

The measured dark-field CTF values for all three resists are well below the levels expected from simulation, even for the “high-resolution” resists. One possible explanation for this difference is flare. If the flare is significantly larger than predicted, this might explain at least part of the difference between measured and simulated curves. This is investigated in Sec. V by measuring the CTF for both dark-field and bright-field cases. A second possible explanation is aberrations. The simulation results in Fig. 4 showed that aberrations have a strong effect on the CTF. Previous results⁸ have shown that the MET optic exhibits some drift in aberration level. Although a few low-order aberration terms have been characterized lithographically, in many cases it is difficult or impossible to accurately obtain such information for all aberrations. If the aberration levels have changed significantly for the worse since the interferometry and lithographic characterization experiments that provided data for the simulation were performed, this could explain the difference between simulated and measured CTFs. This possibility is investigated in Sec. VI by measuring the orientation dependence of the CTF in order to detect any effects of nonrotationally symmetric aberrations. One additional explanation is simply the finite resolution of the resist due to a variety of factors such as acid diffusion length and chemical composition.¹⁰

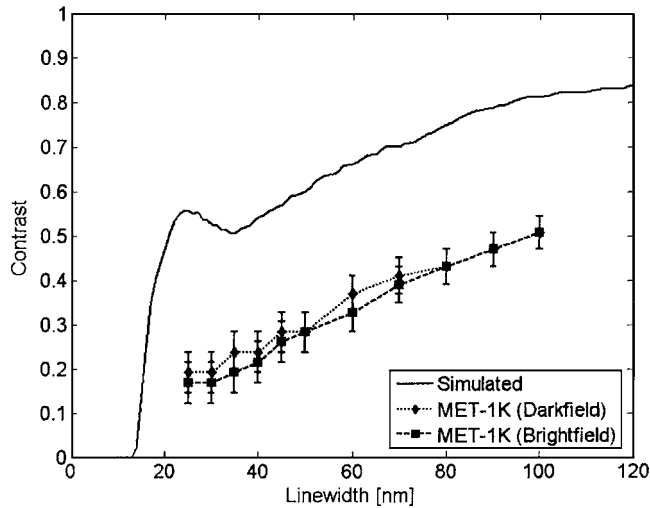


FIG. 6. Comparison of dark-field and bright-field CTFs. The error bars represent the uncertainty due to finite exposure dose step size in the focus-exposure matrix used in the experiment.

V. COMPARISON OF BRIGHT-FIELD AND DARK-FIELD CONTRAST TRANSFER FUNCTIONS

In order to investigate the potential effect of flare on the CTF, measurements were performed using both a bright-field mask (multilayer coatings exposed over the majority of the mask area) and a dark-field mask. If flare is a significant factor in the contrast transfer function, it would be expected that the bright-field case would exhibit decreased CTF values as compared with the dark-field case. The same resist processing and illumination parameters described in Sec. IV were used in these experiments. The results for both measurements using Rohm and Haas MET-1K resist are shown in Fig. 6. The error bars on the measured curves in Fig. 6 represent the uncertainty due to finite exposure dose step size in the focus-exposure matrix used in the experiment.

The fact that there is no significant difference (i.e., no difference outside the error bars) between the two curves indicates that flare is most likely not a dominant factor in the CTF measurements. Moreover, independent flare measurements¹¹ have shown the flare to be in good agreement with predicted values, thus leading to a high level of confidence in the flare values used for the aerial-image modeling.

VI. ORIENTATION DEPENDENCE OF CONTRAST TRANSFER FUNCTION

The CTF was measured for four different orientations (0° , 90° , -45° , and 45°) in order to investigate the possibility that a significant amount of aberration was introduced into the system between the interferometry measurements and the CTF measurements. These measurements were conducted using elbow patterns, as shown in Fig. 7. The modulation present in the resist is observed for each pattern orientation for adjacent elbow patterns. The fact that the elbow patterns are very close to each other ensures that any sources of variation (focus or exposure dose nonuniformity, for example)

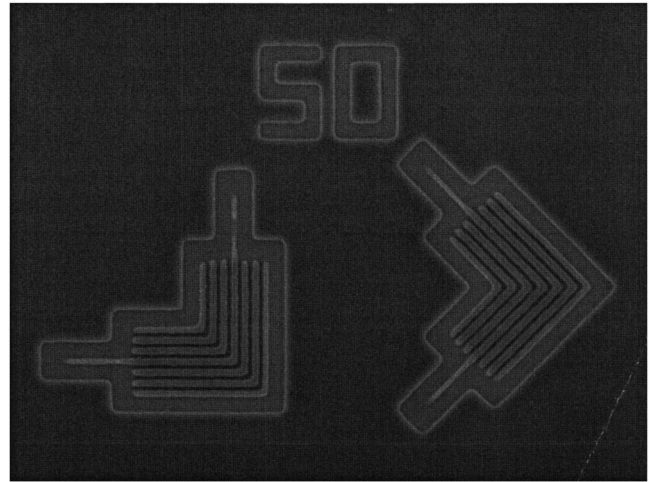


FIG. 7. Example of elbow patterns used to measure orientation dependence of contrast transfer function. The nested features in this structure consist of 50 nm lines and spaces. Similar structures with line and space widths ranging from 20 to 100 nm were used in the measurements.

should be negligible. If any nonrotationally symmetric aberrations are present in significant levels, the measured CTF values for the different orientations should show significant variation. However, it should be noted that this experiment is not able to detect the effect of rotationally symmetric aberrations such as defocus or spherical aberration. We note that the experiment included a complete focus-exposure matrix and that the CTF measurements are based on the optimal focus value as found on the printed wafer, thus focus is not expected to be an issue.

The experiment was conducted using Rohm and Haas MET-1K (XP 3454C) resist. Annular illumination was used with $\sigma_{\text{inner}}=0.3$ and $\sigma_{\text{outer}}=0.7$. The results of the experiment are shown Fig. 8. The error bars in Fig. 8 represent the un-

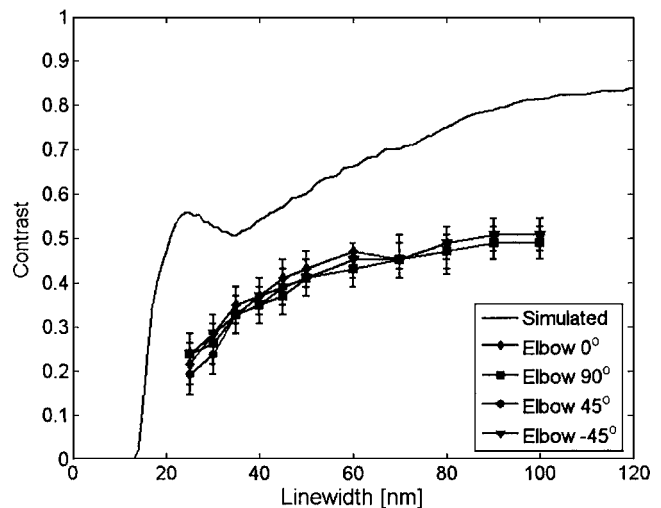


FIG. 8. Contrast transfer function as measured using elbow patterns. Simulation results (including effects of aberrated wave front) are shown along with measurements for four different orientations. The error bars represent the uncertainty due to finite exposure dose step size in the focus-exposure matrix used in the experiment.

certainty due to finite exposure dose step size in the focus-exposure matrix used in the experiment. The fact that there is little variation seen (no variation outside the error bars) between the CTF curves for the four orientations shown in Fig. 8 is an evidence that at least nonrotationally symmetric aberrations do not play a significant role in the measured CTF. This indicates that some other factors may be at work, the most likely of which is limited photoresist resolution.

VII. CONCLUSIONS

The CTF for the MET optic at LBNL was measured using a photoresist clearing method and compared to predicted values from simulation. These simulations included measured aberrations and flare present in the optical system. The measured CTF was significantly lower than the simulated values through pitch. In addition, a strong dependence on photoresist type was observed. The measured CTF correlates well with the observed photoresist resolution limits. The effects of flare on the CTF were studied by measuring the CTF for both dark-field and bright-field mask patterns. No significant difference was observed between the two measurements, indicating that flare is not playing a dominant role in the measured CTF for the MET system. In addition, the effect of nonrotationally symmetric aberrations was investigated by measuring the CTF for four different feature orientations. Again, no significant differences were observed in the measurements. This indicates that nonrotationally symmetric aberrations are not present in sufficient levels to affect the CTF. Because the level of spherical aberration was measured lithographically and accounted for in the CTF simulations, we believe the most likely cause for the discrepancy between measured and predicted contrasts to be the limited resolution of the resist.^{10,12} However, this work demonstrates that important information about the optical system may be obtained in spite of the nonlinear response of the photoresist used as a detector in the experiments.

ACKNOWLEDGMENTS

Many thanks are due to the excellent technical staff at CXRO, including Ken Goldberg, Paul Denham, Brian Hoef, and Erik Anderson. Thanks are also due to Kim Dean of SEMATECH for her support of this research, and to Robert Brainard of Rohm and Haas and Greg Wallraff of IBM for resist support. Lawrence Berkeley National Laboratory is operated under the auspices of the Director, Office of Science, Office of Basic Energy Science, of the U.S. Department of Energy. This work was funded by Advanced Micro Devices, Applied Materials, Atmel, Cadence, Canon, Cymer, DuPont, Ebara, Intel, KLA-Tencor, Mentor Graphics, Nikon Research, Novellus Systems, Panoramic Technologies, Photronics, Synopsis, Tokyo Electron, and the UC Discovery Grant.

- ¹P. Naulleau, K. A. Goldberg, E. Anderson, K. Bradley, R. Delano, P. Denham, B. Gunion, B. Harteneck, B. Hoef, H. Huang, K. Jackson, G. Jones, D. Kemp, J. A. Liddle, R. Oort, A. Rawlins, S. Rekawa, F. Salmassi, R. Tackaberry, C. Chung, L. Hale, D. Phillion, G. Sommargren, and J. Taylor, *Proc. SPIE* **5374**, 881 (2004).
- ²P. Naulleau, K. A. Goldberg, E. Anderson, J. P. Cain, P. Denham, K. Jackson, A.-S. Morlens, S. Rekawa, and F. Salmassi, *J. Vac. Sci. Technol. B* **22**, 2962 (2004).
- ³P. P. Naulleau, K. A. Goldberg, E. H. Anderson, J. P. Cain, P. Denham, B. Hoef, K. Jackson, A. Morlens, and S. Rekawa, *Proc. SPIE* **5751**, 56 (2005).
- ⁴P. P. Naulleau, K. A. Goldberg, P. Batson, J. Bokor, P. Denham, and S. Rekawa, *Appl. Opt.* **42**, 820 (2003).
- ⁵J. Goodman, *Introduction to Fourier Optics*, 2nd ed. (McGraw-Hill, New York, 1996), Chap. 6.
- ⁶A. Grassman and H. Moritz, *J. Vac. Sci. Technol. B* **10**, 3008 (1992).
- ⁷J. A. Hoffnagle, W. D. Hinsberg, M. I. Sanchez, and F. A. Houle, *Opt. Lett.* **27**, 1776 (2002).
- ⁸K. A. Goldberg, P. Naulleau, P. Denham, S. B. Rekawa, K. Jackson, J. A. Liddle, and E. H. Anderson, *Proc. SPIE* **5374**, 64 (2004).
- ⁹G. M. Wallraff, D. R. Medeiros, M. Sanchez, K. Petrillo, W. Huang, C. Rettner, B. Davis, C. E. Larson, L. Sundberg, P. J. Brock, W. D. Hinsberg, F. A. Houle, J. A. Hoffnagle, D. Goldfarb, K. Temple, S. Wind, and J. Bucchignano, *J. Vac. Sci. Technol. B* **22**, 3479 (2004).
- ¹⁰J. P. Cain, P. Naulleau, and C. J. Spanos, *Proc. SPIE* **5751**, 301 (2005).
- ¹¹J. P. Cain, P. Naulleau, and C. J. Spanos, *Proc. SPIE* **5751**, 741 (2005).
- ¹²S. H. Lee, D. A. Tichenor, and P. Naulleau, *J. Vac. Sci. Technol. B* **20**, 2849 (2002).